3-D PRINTING BASED PRODUCTION OF HEAD AND NECK MASKS FOR RADIATION THERAPY USING CT VOLUME DATA: A FULLY AUTOMATIC FRAMEWORK

Shuqing Chen[1,2], Yanye Lu[1,3], Christian Hopfgartner[2,4], Michael Sühling[2], Stefan Steidl[1], Joachim Hornegger[1], Andreas Maier[1]

[1]Pattern Recognition Lab, Department of Computer Science,
Friedrich-Alexander-Universität Erlangen-Nürnberg, Germany
[2]Research & Development, Computed Tomography & Radiation Oncology,
Imaging & Therapy Systems, Siemens Healthcare GmbH, Germany
[3]Department of Biomedical Engineering, Peking University, Beijing, China
[4]ISO Software Systeme GmbH, Germany

ABSTRACT

In this study, we proposed a fully automatic framework to construct and produce immobilization masks for radiation therapy of head/neck. This method uses 3-D printing technology along with image analysis approaches based on 3-D CT image data, which consists of two important aspects: facial model construction and facial features recognition. The facial model construction dedicates to extract the skin surface of head/neck/shoulder. After that the facial features are recognized automatically based on deformable shape models. The results were evaluated quantitatively using real CT data and ground truth, which indicates the robustness and the practical applicability of the framework.

Index Terms – 3-D printing, immobilization mask, atlas registration

1. INTRODUCTION

In radiotherapy treatment it is necessary to ensure the precision of the irradiation for minimizing the radiation dose, in which patient's set-up during the whole therapy and patient's movement during the treatment are two precision relevant factors [1]. Currently, immobilization masks are widely used in head/neck cancer therapy for restricting the patient's movements during the therapy. Two methods are mostly used for producing the immobilization masks: thermoplastic mesh and wet plaster bandages. For both methods, the immobilization masks are produced individually and manually by mould technician or radiographer. Patients have to visit the moulding room of the radiotherapy department for the production of the immobilization masks, which is time consuming due to multiple hospital visits. According to the study of Cancer Research UK[12], each moulding process takes around half an hour, which would bring inconvenience to patients and take more costs for hospitals. Furthermore, the moulding process that covering the face with the mask material to the end, is uncomfortable and distressing [2], especially for the patients with claustrophobia or skin cancer on face. Apart from the inconvenience caused by the moulding procedure, most of the reference marks are placed on the mask manually after the mask production, which might lead to unexpected inaccuracy. In addition, the possible movements of unfixed patients during the moulding procedure could also make the mask inaccurate. In conclusion, the current technology for mask production is time-consuming, uncomfortable, and inaccurate.

Since CT scans are required in the radiation therapy treatment routine, one possible improvement is to construct the radiotherapy immobilization masks using CT image data for image analysis, then produce the masks automatically with 3-D printing technology using the analyzed results. Several researches [2][3] verified that the 3-D printed immobilization masks using image data derived from medical diagnosis devices are feasible and valuable. However these methods are neither fully automatic nor accurate enough. To solve these problems, we proposed a fully automatic framework to construct and produce immobilization masks for radiation therapy of head/neck, which uses automatic segmentation approaches along with atlas registration. We performed several experiments to investigate the feasibility of our method. To the best of our knowledge, this is the first framework of immobilization mask production with automatic recognition and automatic removal of facial features.

2. METHODS

In order to construct and produce immobilization masks using CT image data and 3-D printing technology, it is necessary to extract the 3-D surface of interested anatomy regions. The valuable anatomy regions, such as forehead that are necessary for the immobilization, should be segmented exactly. Conversely, some useless anatomic

regions such as eyes, mouth, ears, and nostrils should be cut off from the face mask to comfort the patients. Thus, it is necessary to recognize facial features automatically and allow the optional function of removal for the end-user. In this study, we used atlas registration [4] for this purpose.

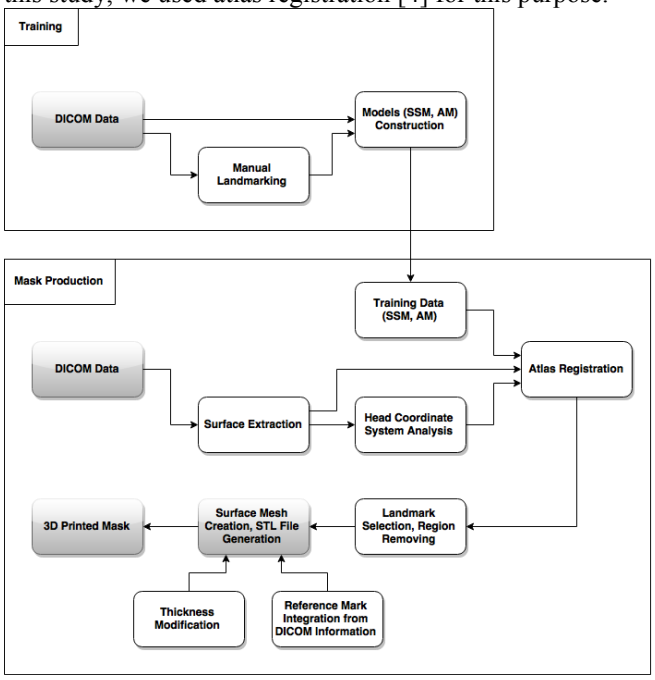

Fig. 1. The general procedure flow chart. SSM: Statistical Shape Model. AM: Appearance Model

The general procedure of the method is shown in Fig. 1. First of all, a statistic facial model with anatomical landmarks is constructed using the CT image data from the training data set. For a new image, the 3-D surface is obtained from the surface extraction. Subsequently we achieve the positions of the anatomical landmarks for this new image by aligning the statistic facial model on the extracted surface using atlas registration. After mapping the registration results on the segmented surface, the anatomical regions for optional removal are labeled automatically. Finally, a surface mesh is generated and saved as .stl (standard tessellation language) file, which can be used for editing and 3-D printing.

2.1. Facial Model Construction

The facial model in this study consists of a statistical shape model and an appearance model. The construction procedure contains the following steps:

1. Original volume images are converted into meshes.
2. 25 landmarks are designed and marked manually on the 3-D surfaces of training images.
3. Procrustes Analysis [5] is used for the point cloud alignment.
4. The method introduced by Cootes et al. in [6] is applied to generate our facial statistical shape model.
5. A non-linear intensity profile model described in [7] is generated as facial appearance model.

2.2. Surface Extraction

As mentioned before, the 3-D surface of the anatomy regions of interest of a new image must be extracted for the mask production using 3-D printing technology. The analysis of original CT images shows, that the challenges in our surface segmentation are: similar HU values between the human head soft tissues, external structure, complex outer contour and artifacts. After comparing different segmentation methods, a segmentation workflow is outlined as follows:

1. The grayscale image is converted into a binary image using Otsu's thresholding [8].
2. The head object is separated from the head support object using morphologic opening filter.
3. The OKE contour extraction method [9, 10] is applied for each slice to extract and fill the object contours. This method is a variant of the chain code method. It encodes binary image into direction code map by applying 8 direction masks. Then object contour can be extracted by tracing contour pixels on the direction code map.
4. The objects are classified to elliptic and non-elliptic objects with a shape descriptor [11] combining object circumference and area. As result of the segmentation, head support tools or instruments which do not have an elliptic shape are removed.

2.3. Facial Features Recognition

Facial features can be mapped onto the segmented facial surface automatically by using atlas registration, which can be divided into two steps:

1. Initialization/Coarse Alignment -- The facial model is placed to an initial pose, such as the volume center.
2. Search/Alignment -- The active shape model introduced by Cootes et al. in [6] is applied to refine the alignment to achieve the optimum. Because the head could sway in different directions with varied angles, multiple start poses are applied to enhance the accuracy of the registration.

3. RESULTS AND EVALUATION

In this work, we employed 10 volume images from anonymized patients to evaluate the segmentation accuracy and the accuracy of facial feature recognition.
The ground truth is generated by manually annotating the edge points in slice images to evaluate the accuracy of the segmentation method. The segmentation error is derived by calculating the closest distance among annotation points and automatically extracted contours. As shown in Table 2 the

average segmentation error is 0.4mm with a maximum error of 0.64mm.

Image no.	Mean error (mm)	Std. dev.
1	0.42	0.27
2	0.43	0.15
3	0.64	0.09
4	0.28	0.05
5	0.37	0.15
6	0.41	0.10
7	0.36	0.15
8	0.38	0.05
9	0.37	0.07
10	0.38	0.08

Table 2. Evaluation of segmentation accuracy with 10 patient volume images, each image contains more than 340 slices.

The volume images are employed as training data to generate the statistical shape model as well. 25 landmarks are annotated manually using the method described in Section 2.1. Based on the landmarks, a statistical shape model is generated (see Fig. 2). Table 3 shows the most significant eigenvalues. The shape variations are demonstrated in Fig. 3. Assumed that a reference mark is defined in radiotherapy plan between the eyebrows, Fig. 4 illustrates an automatic generated final surface mesh after the surface extraction, the facial features removal, and the integration of the reference mark from the DICOM data of the radiotherapy plan.

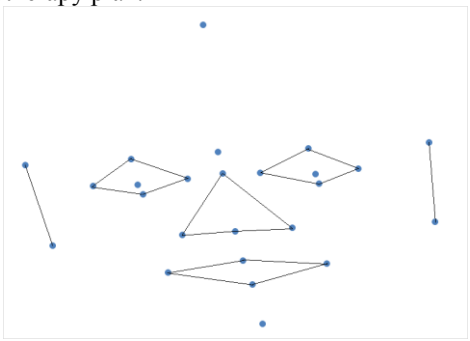

Fig. 2. The mean shape projected onto XZ plane in patient coordinate system

Eigenvalue	$\frac{\lambda_i}{\lambda_T} \cdot 100\%$
λ_1	23.83%
λ_2	18.49%
λ_3	17.53%
λ_4	15.03%
λ_5	8.21%
λ_6	5.89%
λ_7	4.72%
λ_8	3.42%
λ_9	2.88%

Table 3. Eigenvalues of the covariance matrix derived from the training samples. λ_T is the sum of all eigenvalues.

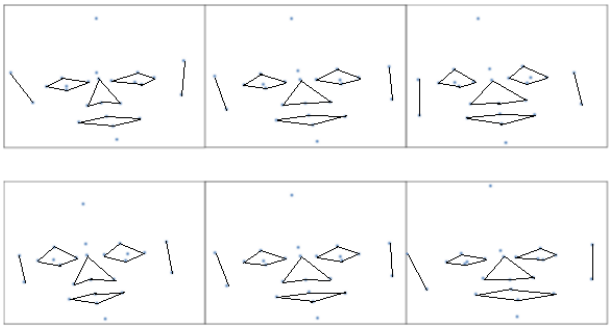

Fig. 3. Shape change due to individual variation of the two largest principal components of the shape model. The vector **b** defines the weight for each eigenvector. First row: the weight b_1 between $-3\sqrt{\lambda_1}$ and $3\sqrt{\lambda_1}$. Second row: the weight b_2 between $-3\sqrt{\lambda_2}$ and $3\sqrt{\lambda_2}$.

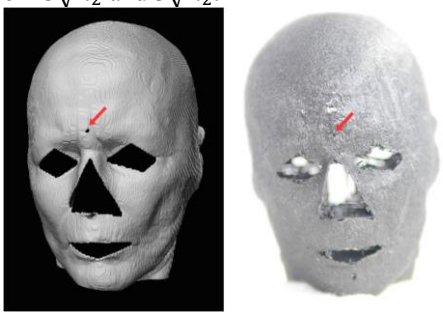

Fig. 4. Left: final surface mesh; Right: printed mask; Arrow: the reference mark.

In order to evaluate the accuracy of the atlas registration, a cross validation test has been made (see Table 4). For each test, the test data is aligned with the statistical shape model. The Euclidian distance between aligned landmarks and their corresponding manual annotations is defined as registration error. As shown in Fig. 5, the mean errors of cross validation trails are between 6mm and 14mm.

4. DISCUSSION AND CONCLUSION

In this work, we proposed a fully automatic framework to construct and produce immobilization masks for radiation therapy of head/neck, which consists of a segmentation module and a facial feature recognition module. The segmentation module can precisely extract the 3-D face. In the facial feature recognition module, an atlas-based registration is applied to recognize facial landmarks, which can enable user editing and cutting facial anatomy region on the segmented surface.

The accuracy of the proposed segmentation method has been evaluated. The evaluation results show that the segmentation method has a very low segmentation mean errors of 0.4mm, which enables a very high accurate mask production.

The accuracy of the feature recognition has been evaluated with cross validation scenarios as well. The results show a mean registration error of 11.78mm, which

has been proven to be adequate errors for providing an initial position of landmarks for editing purpose (as shown in Fig. 4).

Test no.	Training data index	Test data index	Mean error (mm)	Std. dev.
1	Image 2-10	1	13.57	8.87
2	Image 1, 3-10	2	11.45	8.16
3	Image 1-2, 4-10	3	13.70	7.57
4	Image 1-3, 5-10	4	10.82	6.18
5	Image 1-4, 6-10	5	12.99	8.58
6	Image 1-5, 7-10	6	14.05	7.18
7	Image 1-6, 8-10	7	14.48	7.41
8	Image 1-7, 9-10	8	11.41	7.29
9	Image 1-8, 10	9	9.24	5.33
10	Image 1-9	10	6.05	3.14

Table 4. Cross validation test scenarios

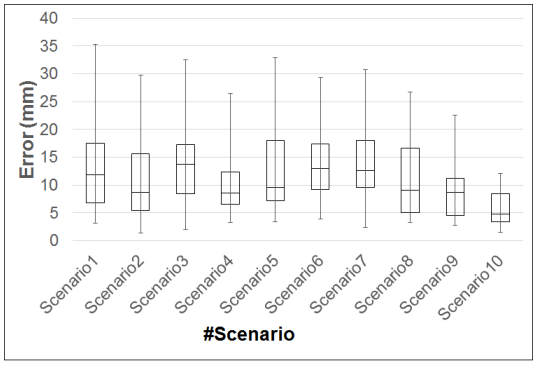

Fig. 5. Evaluation results of the cross validation

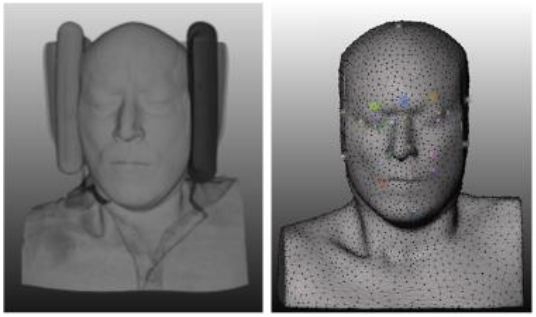

Fig. 6. Test result of image with invisible ears. Left: original image. Right: registration result.

In addition, the feasibility of the atlas registration has been verified with the image that lacks parts of anatomic regions. As shown in the left column of Fig. 6, the patient's ears are hidden in the head support. The right column of Fig. 6 shows that the results of the atlas registration are also acceptable under this circumstance.

In conclusion, the results indicate the feasibility and the robustness of our automatic construction and production framework, which has the potential features of time-saving, comfortable for patient and friendly for hospital staff.

5. ACKNOWLEDGMENT

The authors gratefully acknowledge funding support from the Siemens CR. The authors also gratefully acknowledge funding of the Research Training Group 1773 Heterogeneous Image Systems by the German Research Foundation (DFG).

Disclaimer: The concepts and information presented in his paper are based on research and are not commercially available.

6. REFERENCES

[1] A. Dutreix, "When and how can we improve precision in radiotherapy?" , *Radiotherapy and Oncology*, 2(4):275-292, 1984.

[2] M. Fisher, C. Applegate, M. Ryalat, S. Laycock, M. Hulse, D. Emmens, and D. Bell, "Evaluation of 3D printed immobilization shells for head and neck IMRT," *Open Journal of Radiology*, 04(04):322-328, 2014.

[3] S.D. Laycock, M. Hulse, C.D. Scrase, M.D. Tam, S. Isherwood, D.B. Mortimore, D. Emmens, J. Patman, S.C. Short, and G.D. Bell, "Towards the production of radiotherapy treatment shells on 3D printers using data derived from DICOM CT and MRI: preclinical feasibility studies," *Journal of Radiotherapy in Practice*, pp. 92-98, July 2014.

[4] M. Unberath, A. Maier, D. Fleischmann, J. Hornegger, and Rebecca Fahrig, "Open-source 4D Statistical Shape Model of the Heart for X-ray Projection Imaging", *Proceedings of the ISBI*, Brooklyn NY, pp. 739-742, 2015.

[5] I.L. Dryden, and K.V. Mardia, *Statistical Shape Analysis*, John Wiley & Sons, Chichester, 1998.

[6] T.F. Cootes, C.J. Taylor, D.H. Cooper, and J. Graham, "Active shape models: Their training and application," Computer Vision and Image Understanding 61(1):38-59, January 1995.

[7] T. Heimann, *Statistical Shape Models for 3D Medical Image Segmentation,* VDM-Verlag Müller, 2009.

[8] N. Otsu, "A threshold selection method from gray-level histograms," *IEEE Transactions on Systems*, 9(1):62-66, Jan 1979.

[9] H.A. Nour Eldin, *Automatisierungstechnik und Technische Kybernetik ATK Institutsbericht 1978-1999,* Bergische Universität GH Wuppertal, 2000.

[10] W. Wei, *Entwicklung und Verifikation von Verfahren zur automatischen Bestimmung eines Kalibrierkörpers innerhalb der Volumendaten eines Magnetresonanztomographen,* Master's thesis, FH Gelsenkirchen, 2006.

[11] L. O'Gorman, M.J. Sammon, and M.Seul, *Practical Algorithms* for Image Analysis, Cambridge University Press, 2008.

[12] Cancer Reserach UK, London: Radiotherapy moulds, http://www.cancerresearchuk.org/about-cancer/cancers-in-general/treatment/radiotherapy/external/plan/radiotherapy-moulds, October 2014